Straylight testing during EQM
B. Swinyard

0 Scope

In this note I briefly report on the ambient radiation environment seen during Herschel EQM testing at Ottobrunn in September/October 2005.

1 Test description

Following cooler recycle a load curve was taken once the evaporator temperature had settled to a steady state with the cryostat lid cooled to below 10K. The test procedure was carried out between 13:11 and 13:53 on the 25 October 2005. The scripts used were SPIRE-IMT-LC1-P and SPIRE-IMT-LC2-P and the OBSIDs were B000003D and B000003E. During the loadcurve the evaporator temperature was ~284 mK.

2 Data analysis

The loadcurve data were analysed using the standard method whereby first the resistance of the bolometer thermistors is deduced from the measured voltage across the thermistor and knowledge of the load resistors and bias voltages. From the thermistor resistance we can establish the temperature of the thermistor from the calibration established at JPL before delivery of the BDAs. From the temperature we can estimate the absorbed power in the bolometer by taking the difference in temperature between the sink temperature measured close to the bolometers with an identical thermistor not exposed to the ambient radiation, again using the JPL calibration for the thermal conductance of bolometer. Finally we can convert absorbed power on the bolometer to the power incident at the SPIRE focal plane using the optical efficiency of the detectors and an estimate of the instrument transmission and etendue as given in table 1. During ILT the product of etendue and transmission was shown to be low by up to 30% for the CQM instrument; the estimated incident power may therefore be higher by this figure.

Parameter	Where derived from	Value
Instrument spectral bandpass	Measurements of individual filters and feedhorn specification	Average transmission 0.55 between 427 and 603 μm
Detector optical efficiency	Taken from the BDA EIDP	Varies
Etendue (AΩ)	Theoretical expected for single mode	λ^2
Expected cold stop efficiency	Optical model	0.84
Loss due to absorption and scattering from the mirrors	Estimate	$0.99^7 = 0.93$

Table 1: Estimated instrument performance values used for calculating incident power onto SPIRE.

3 Results

Figure 1 shows the estimated power incident at the SPIRE aperture for each pixel in the array in (more or less) their physical order on the array. The same data are shown as an image in figure 2. Figure 3 shows the actual temperature of each pixel; the estimated power incident of the detectors (rather than at the aperture of SPIRE) and the estimated noise at the nominal operating bias. Here I have truncated the y-scale for the power and made it linear so we can see the ambient power on the detectors.

Both the temperature and ambient power show a reasonably large gradient across the array from the “1” column to the “8/9” column; the incident power being about 8 pW at one side of the array and about 6 pW at the other. All the edges of the array appear to have more power incident on them than the centre. Superimposed on this general background some pixels have a large excess power in them - shown as light brown in the image where I have truncated the colour table at ~80 pW so all bright pixels have about the same colour. Two of the pixels have extreme amounts of power apparently falling on them (E2, E4). They are therefore highly non-linear in their response

and the absolute power figure reported here should not be trusted. Especially as the maximum power in the band from even a 300 K source is only ~few hundreds of pW.

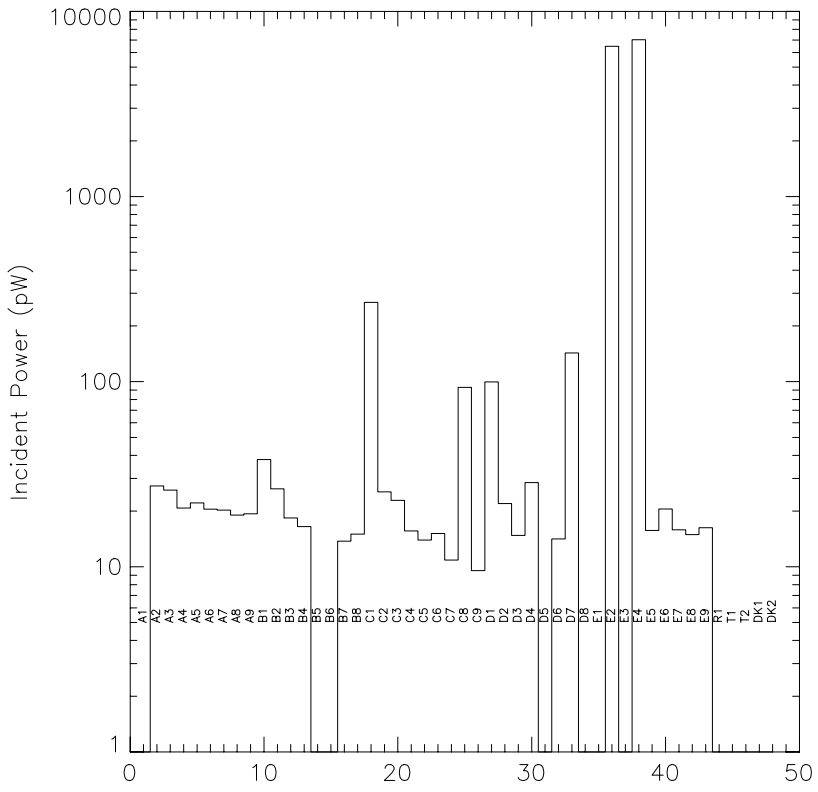

Figure 1: Estimated absorbed power on each pixel in the PLW array during loadcurve B000003D and B000003E with pixels labelled in physical order on the array.

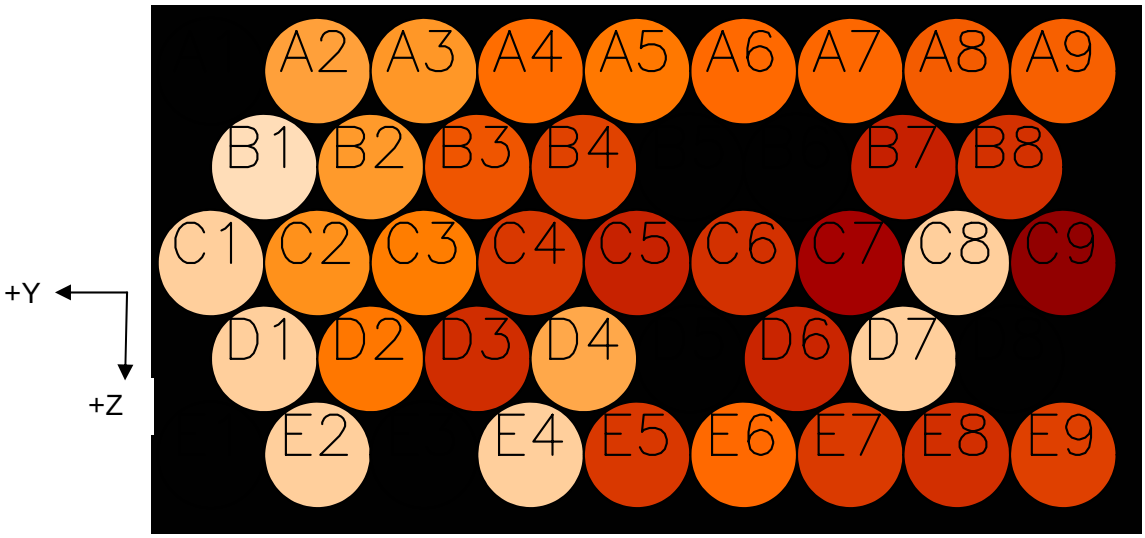

Figure 2: Image of the SPIRE PLW array projected at the SPIRE focal plane showing the distribution of incident power during loadcurve B000003D and B000003E. This is a logarithmic red temperature colour table – lighter colours are more power. The missing pixels - A1, B5, B6, D5, D8, E1 and E3 - are non-operational. The arrows indicate the relative orientation of the array in the Herschel co-ordinate system

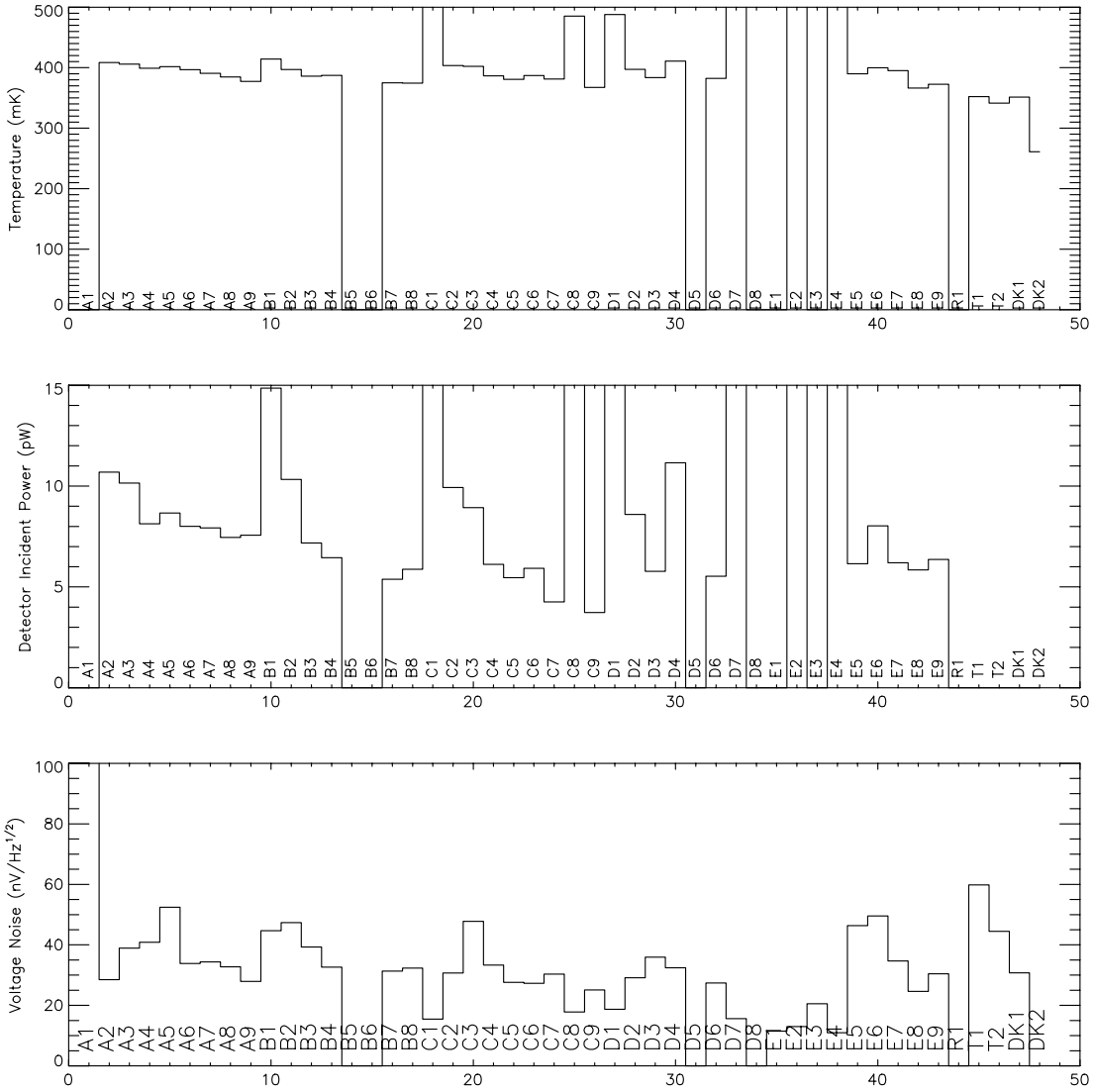

Figure 3: Top – temperature of each pixel, we can use the difference in temperature between the thermistors “T1” and “T2” to estimate the power absorbed onto the bolometers. Middle – the estimated power incident on the detectors after correcting for the optical efficiency of the feedhorns. Bottom – estimated noise at the nominal bias setting seen during the measurement.

4 Comparison with ILT

Figure 4 shows the temperature; incident power on the detectors and noise at operating bias seen during the CQM ILT at RAL. Comparison with the CQM results shows us that the ambient environment in the CQM cryostat is equivalent to a black body of ~15 K (red lines in figure 4). We can see that , apart from some drop off in the last two columns of the array, the power profile across the array is essentially flat and not all similar to that seen during EQM.

Interestingly the noise is seen to go down as the flux on the detectors increases. This is due to a quirk in the QM1 electronics whereby there is excess noise in the offset circuitry and as the power increases the measured voltage decreases and therefore so does the offset and the injected noise. This aside the noise seen under ambient conditions (rather than the very bright pixels) during EQM is essentially the same as seen during ILT and very similar to that expected under flight conditions. The two very brightest pixels in the EQM environment (E2 and E4) have the lowest noise figure. This figure is so low as to indicate that the detectors were effectively behaving as a shorted input to the JFETs as the noise is the same as seen when the detectors are warm.

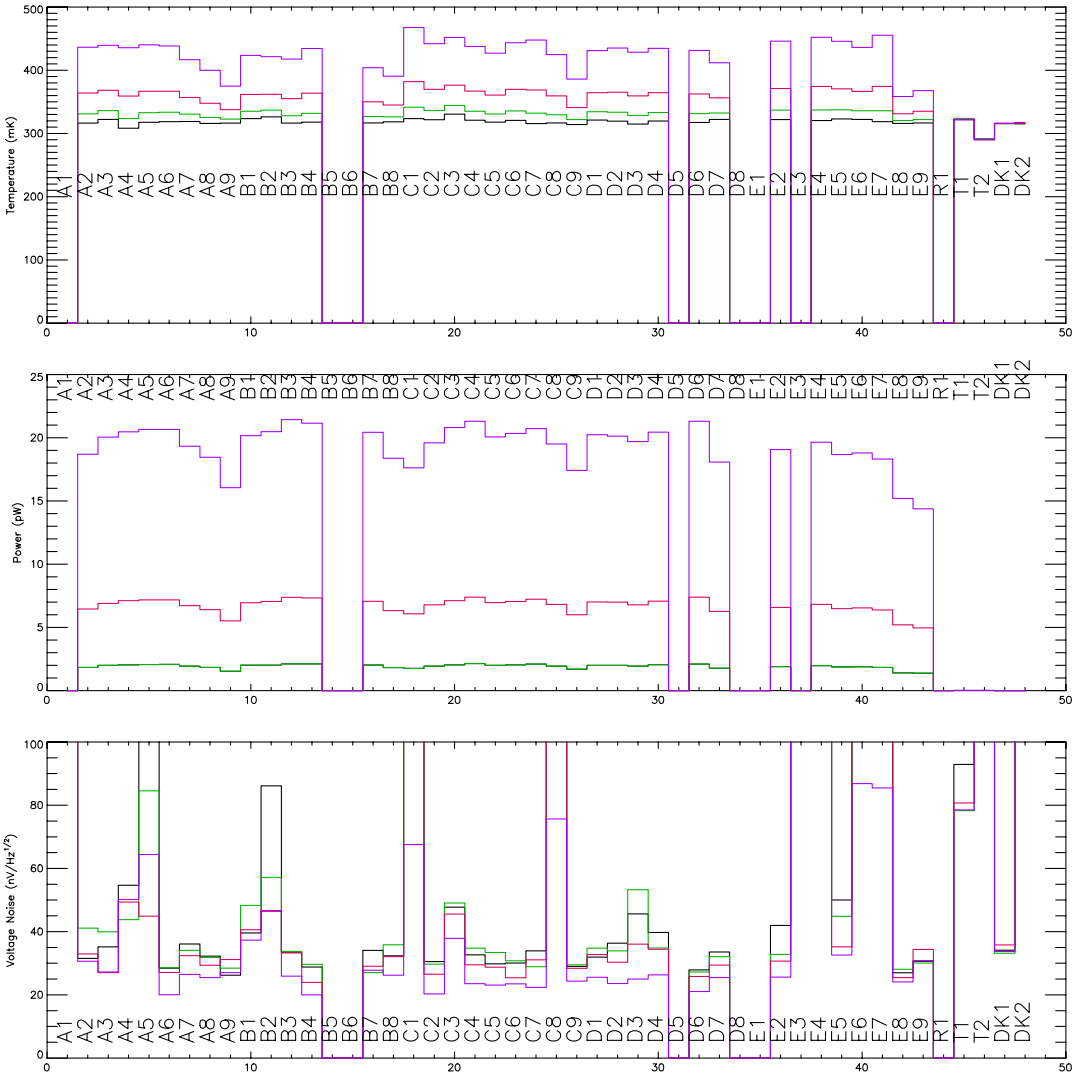

Figure 4: As figure 3 but here the data are from the CQM ILT whilst the instrument is staring at a cold black body set at 6.68K (black), 9.97 K (green), 15K (red) and 25K (purple).

5 Conclusions

To understand the origin of the straylight seen in the EQM cryostat we would need to run a proper optical model. This is beyond the scope of the present document, however we can orientate the situation and offer some clues as to where the light may be originating. Figure 5 shows a sketch of the orientation of the SPIRE PLW as viewed from above the Herschel focal plane. The baffle tube on this instrument model was not coated in absorbing tiles and therefore has a high reflectivity in the sub-mm, the straylight seen is could easily be a glint off the walls of the tube from a high temperature environment. In the case of the saturated detectors (E2 and E4) this must be from a temperature >>77 K as shown in figure 6 – i.e. it must be from a room temperature environment. Although the bright ring of radiation is clearly unacceptable if this were to be present the flight model, we must not ignore the ambient radiaition environment which may not be due to the same source. This represents a straylight level equivalent to the worst case telescope (80 K 4% emissivity) and the source of this must also be found and eliminated or it will severely restrict the sensitivity of SPIRE.

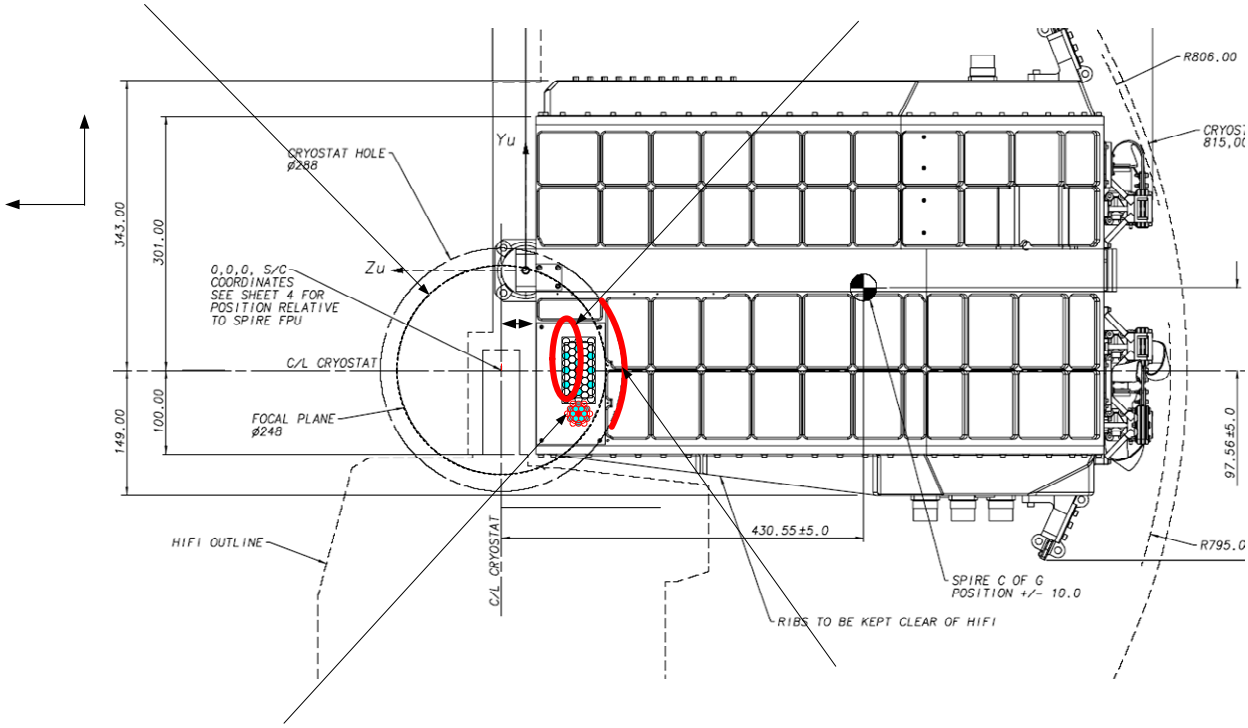

Figure 5: Skectch showing the location of the SPIRE FOV viewed in the –X direction (“above”). The most likely source of the bright ring of radiation is from just outside the field of view in the –Z direction seen in reflection from the un coated SPIRE baffle. The red arc shows a possible location at the hole through the cryostat shields for illustrative purposes only.

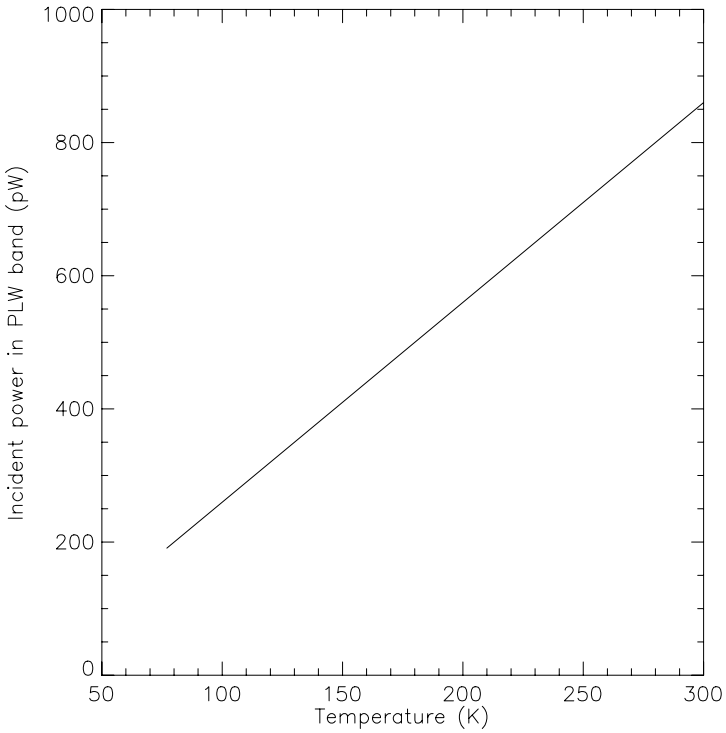

Figure 6: Estimated power incident on a pixel at the SPIRE aperture versus temperature of the emitting source assuming an emissivity of 1. Comparison with figure shows that the brightest part of the straylight in the EQM must be coming from a source >>77 K – essentially it must be from a room temperature source.